Published in final edited form as:

Nat Methods. 2010 May ; 7(5): 387–390. doi:10.1038/nmeth.1452.

Using buoyant mass to measure the growth of single cells

Michel Godin[1,*,2], **Francisco Feijó Delgado**[1,*], **Sungmin Son**[3], **William H. Grover**[1], **Andrea K. Bryan**[1], **Amit Tzur**[4], **Paul Jorgensen**[4,5], **Kris Payer**[6], **Alan D. Grossman**[7], **Marc W. Kirschner**[4], and **Scott R. Manalis**[1,3]

[1] Department of Biological Engineering, Massachusetts Institute of Technology, Cambridge, MA 02139, USA

[3] Department of Mechanical Engineering, Massachusetts Institute of Technology, Cambridge, MA 02139, USA

[4] Department of Systems Biology, Harvard Medical School, Boston, MA 02115, USA

[6] Microsystems Technology Laboratory, Massachusetts Institute of Technology, Cambridge, MA 02139, USA

[7] Department of Biology, Massachusetts Institute of Technology, Cambridge, MA 02139, USA

Abstract

We used a suspended microchannel resonator (SMR) combined with picoliter-scale microfluidic control to measure buoyant mass and determine the 'instantaneous' growth rates of individual cells. The SMR measures mass with femtogram precision, allowing rapid determination of the growth rate in a fraction of a complete cell cycle. We found that for individual cells of *Bacillus subtilis*, *Escherichia coli*, *Saccharomyces cerevisiae* and mouse lymphoblasts, heavier cells grew faster than lighter cells.

Understanding how the rate of cell growth changes during the cell cycle and in response to growth factors and other stimuli is of fundamental interest. Over the decades, various approaches have been developed for describing cellular growth patterns but different studies have often reached irreconcilable conclusions, even for the same cell types. The debate has focused on whether cells grow at a constant rate (linear) or at a rate that is dependent on their size (exponential), although more complex growth curves have also been suggested.

Correspondence should be addressed to S.R.M.(scottm@media.mit.edu).

*co-1st authors

[2]Present address: Department of Physics, University of Ottawa, Ottawa, Ontario K1N 6N5, Canada

[5]Present address: Donnelly Centre for Cellular and Biomolecular Research, University of Toronto, Toronto, ON M5S 3E1, Canada

AUTHOR CONTRIBUTIONS

M.G. developed the trapping method, F.F.D. developed the model, M.G. and F.F.D. conducted experiments on bacteria, W.H.G. and A.K.B. adapted the method and conducted experiments on yeast, and S.S. adapted the method and conducted experiments on mouse lymphoblasts. K.P. fabricated the devices used for experiments on mouse lymphoblasts. All authors contributed to designing of the experiments and writing of the manuscript.

COMPETING FINANCIAL INTEREST

The authors declare competing financial interests.

S.R.M. isaco-founder of Affinity Biosensors and declares competing financial interests.

The mean dry mass accumulation of *E. coli* has been reported as increasing linearly[1] and cell length growth described as bilinear[2], bilinear and trilinear[3], and exponential[4]. The size of budding yeast *Saccharomyces cerevisiae* has been reported to increase exponentially by some approaches[5],[6], but to have a non-exponential and cell cycle dependent growth curve by others[7]. For mammalian cells, volume measurements have shown linear growth for rat Schwann cells[8] and exponential growth with a varying rate constant for mouse lymphoblast cells[9]. Several factors may contribute to the discrepancies between different growth models: i) cells are minute, irregularly shaped objects, ii) proliferating cells increase their size only by a factor of two, so distinguishing between different cell growth models with mathematical rigor requires highly precise measurements, iii) a wide variety of methods have been used to measure growth, including approaches that average across populations as well as those that monitor individual cells, and iv) a cell's size includes both volume and mass, which can change at different rates.

While both mass and volume are important parameters, mass is more fundamentally related to cell growth than is volume. Volume can change disproportionately to mass, thereby altering a cell's density. In cells without rigid cell walls, volume can rapidly change in response to osmotic stresses, while even in cells with cell walls, the size of low-density intracellular vacuoles can change to alter the density of cells[10]. Fundamentally, cell growth is the creation of new biomass, the polymerization of small molecules into the lipids, proteins and RNA that make up the membrane, cytoplasm and organelles. But most research into cell size and growth has focused on volume, for lack of methods to measure the mass of individual cells.

An ideal method for measuring cell growth rates would directly and continuously monitor the mass and volume accumulation of single unperturbed cells with high precision. In recent years, optical microscopy has been the closest match to this ideal[3],[5],[11], but volume determination by microscopy has lacked the precision to conclusively distinguish between cell growth models. Potential alternatives include using fluorescent protein reporters that are correlated with cell size[5], or using phase microscopy to measure dry mass during cell growth[11]. Here we describe a system that can precisely monitor the growth of single cells in terms of buoyant mass and show that bacteria, yeast and mammalian lymphoblast cells grow at a rate that is proportional to their buoyant mass. Buoyant massis defined by $m_{\text{buoyant}} = V(\rho_{\text{cell}} - \rho_{\text{fluid}})$ where ρ is density and V is cell volume. It is dependent on the amount of biomassin the cell, most of which is denser than water, and so is analogous to the dry mass of the cell.

We developed a dynamic fluidic control system that enables the buoyant mass of cells as small as bacteria and as large as mammalian lymphocytes to be repeatedly measured with a suspended microchannel resonator (SMR). The SMR consists of a vacuum packed hollow microcantilever beam containing an embedded fluidic microchannel and is capable of weighing nanoparticles, bacterial cells, and sub-monolayers of adsorbed proteins with femtogram resolution (1 Hz bandwidth)[12]. As individual cells transit the microchannel, a shift in the resonant frequency of the SMR is observed that corresponds to the buoyant mass of the cell. We implemented a feedback algorithm that reverses the direction of fluid flow upon detecting a cell transiting through the SMR, thereby reintroducing the cell into the

cantilever (Figs. 1a,b). Continuously alternating flow direction creates a dynamic trap that allows for consecutive buoyant mass measurements of the same cell. Since the cell fully exits the SMR prior to flow reversal, the baseline resonant frequency is acquired after each measurement, allowing compensation for drift arising from temperature variations or accretion on the walls of the microchannel. Dilute cultures of non-adherent cells in any desired growth medium can be loaded directly into the system.

The dynamic trap is very stable when measuring polystyrene particles that are less than half the size of the channel height (3–15μm). We trapped such particles for more than 20 hours (>32,000 measurements) (Supplementary Fig. 1). Sample concentration was the main limiting factor of the trapping duration. Low concentrations ($\leq 10^7$ ml^{-1}) decrease the probability of additional particles randomly drifting into the cantilever and becoming trapped along with the particle being measured. The maximal trapping duration for cells was typically shorter than for polystyrene particles and was dependent on the cell type. On average, *E. coli* and *B. subtilis* could be trapped for 500 sec and 300 sec, respectively, before being lost. Yeast and L1210 mouse lymphoblast cells could be trapped in excess of 30 minutes in a similar system as bacteria but with larger SMR channels. When living cells were trapped, growth was observed from the increasing amplitude of the resonant frequency peaks (Fig. 1c). Trapped cells are in an open system, as the suspended microchannel is in constant contact with the larger inlet and outlet channels (Fig. 1a), which act as reservoirs of nutrients. Diffusion and convection prevent local depletion of nutrients by the growing cell. Variability in the peak amplitudes (Fig. 1c) limits the precision of this method and is mainly due to the trapped cell taking different flow paths as it turns the corners at the cantilever tip. Different flow paths, as well as increased interaction with the microchannel walls, may also explain why cells with irregular shapes (e.g. oblong *E. coli* and *B. subtilis*) escape the dynamic trap much more frequently than do polystyrene particles and round cells.

Following conversion of resonant frequency shifts, growth could be observed as steadily increasing buoyant mass, as in a series of trapped *B. subtilis* cells (Fig. 1d). Occasionally, the magnitude of the frequency shifts would instantaneously drop by a factor of two, suggesting that the trapped cell had divided into two daughter cells, one of which had escaped the trap (Supplementary Fig. 2). Adding the poison sodium azide to a culture of *S. cerevisiae* continuously being loaded to the device resulted in a greatly diminished rate of increase in buoyant mass, demonstrating that these increases are indeed due to cell growth(Supplementary Fig. 3).

In order to determine whether growth rate depends on size, we employed a method where the ‘instantaneous’ growth rate was measured by trapping a cell for a period much shorter than the cell’s own life cycle. For each trapping event, a growth rate is determined and associated with the cell’s buoyant mass at the start of the trapping event. By plotting the growth rate versus buoyant mass, we can piece together temporally localized growth rates of several individual cells to determine the size dependency of growth, provided that the measurement errors are below the natural variability. Such a plot does not necessarily depend on knowing the position of each cell in the cell division cycle, although such information could be valuable and may be obtainable in future devices. We sampled cells from exponential phase cultures of *B. subtilis*, *E. coli*, *S. cerevisiae*, and L1210 mouse

lymphoblasts. Growth rates for each cell were determined by performing linear fits to the buoyant mass data from each trapping event. We plotted growth rates against initial buoyant mass for *B. subtilis* (Fig. 2a), *E. coli* (Fig. 2b), *E. coli* grown at low temperature (Supplementary Fig. 4), *S. cerevisiae (*Fig. 2c), and L1210 mouse lymphoblasts (Fig. 2d). A clear trend is observable in all four cell types: heavier cells grow faster than lighter ones. The relationship between cell size and growth rate appeared to be linear and for *B. subtilis* the linear fit extrapolated close to the origin, which is suggestive of a simple exponential growth pattern (Supplementary Table 1).

The buoyant mass ranges displayed in Figure 2 clearly span over twice the lowest values, particularly in the *B. subtilis* data (Fig. 2a). Buoyant masses that are more than twice the smallest size in the population could potentially represent multiple cells simultaneously entering the SMR. The larger SMR used to trap the L1210 cells allows for optical microscope access, providing confirmation that the cells are singlets. Both the devices used for yeast and bacteria are opaque, but the channel cross-section of the SMR used for yeast greatly reduces the likelihood of trapping clustered cells. However, for the bacteria, clustering is possible and some of the larger mass values are almost certainly doublets. Note that while our exponential phase cultures of yeast and mammalian cells were almost entirely composed of single cells when observed under a microscope, both bacteria cultures contained ~20% of non-segregated cells or small clusters (Online Methods). To isolate the single cell events for bacteria, one could consider only those events which have a buoyant mass that is less than twice the minimum buoyant mass, however the presence of clustered cells can give additional information of the growth pattern of the cells: a discontinuity of the growth rate at about twice the value of the lowest buoyant masses would be inconsistent with exponential growth of single bacteria (Supplementary Fig. 5 and Supplementary Table 2).

Although the data for all cell types are inconsistent with simple linear growth, measurement errors and cell-to-cell variation could potentially mask growth rate changes that would identify multiple stages of linear growth during the cell cycle. In order to evaluate the experimental error of the growth rate determination we performed similar trapping experiments with fixed cells (Online Methods). As the growth rate of fixed cells is zero, the deviation from this value provides a measure of the experimental error. The cell-to-cell variability in growth rates is generally greater than the error of the method (Online Methods and Supplementary Fig. 6 for error analysis). That is, the deviations of cells from the fitted curves in Figure 2 are often not due to experimental error, but instead reflect the biological variation in an isogenic population. Cells–even those of the same buoyant mass, but not necessarily at the same cell cycle position–can exhibit different instantaneous growth rates. Previous cell cycle models typically assume that all cells of a given size grow at the same rate[5,13] and a lack of precision in prior methodologies may have prevented growth rate variability from being observed until now. The cells grew well in our microfluidic devices (Supplementary Table 3), suggesting that our system does not alter normal cellular growth, and as we currently have no information on cell cycle position, it is possible that the measured variations reflect cell cycle-dependent changes in growth rate[5,7,9]. A second possibility is that cell growth is variable in a manner that is independent of cell size and cell

cycle position. The source of this variability is unknown, but many transcripts and proteins are subject to stochastic fluctuations in bacteria, yeast and mammalian cells[14], conceivably influencing growth rate consistency. As previously observed[3,4,15,16], we have found single cell growth to be smooth and continuous and do not believe the observed variability occurs within a cell's lifespan (see text below and Fig. 3). Further investigations will be required to uncover the true nature of this variability.

We were occasionally able to trap *B. subtilis* for long enough to allow a full cell cycle (Fig. 3 and Supplementary Fig. 7). Optical access was not available to verify the presence of single cells; however, for all three long-duration traps, the initial buoyant mass value was in the lower end of the distribution of buoyant masses for the *B. subtilis* population (Supplementary Fig. 8). Therefore, it is likely that only a single cell was present for most of the duration of each long trapping event. When fitting curves to the three long trapping events, a simple exponential fit was a better match than linear or bilinear fits, as verified by four different statistical tests. Results from these long-duration traps support the conclusions of the shorter trapping events with *B. subtilis* (Fig. 2a, Online Methods and Supplementary Table 4 for details of curve fitting). Importantly, analysis of the three long trapping events and the ensemble of shorter "instantaneous" trapping events yielded a consistent cellular doubling time for *B. subtilis*, further validating the method and findings previously described. For all the cell types measured in Figure 2, the single cell growth rates were consistent with the population doubling time of exponential phase cultures(Supplementary Table 3).

A model was implemented to describe our experiment and to compare simulated results for linearly and exponentially growing bacterial cells with experimental data, taking into consideration the fact that our system may measure clustered cells. For *B. subtilis*, we found that the trend and the dispersion of the experimental data are well matched by an exponential growth model. For *E. coli*, we were not able to identify the best growth model due to the high variability of the growth rate values (Supplementary Fig. 7, Online Methods and Supplementary Table 5 for model details).

Our finding that growth rate is size dependent suggests that these bacteria, yeast and mammalian cell types must actively balance their growth and division. If growth and division rates were not coordinated in cells with size-dependent growth, cell size variation in the population would continually increase[17], which is not the case. While molecular mechanisms coordinating growth and division have been described in yeast and bacteria[18], such mechanisms have not yet been characterized in mammalian cells.

We envision that our dynamic trapping method for measuring cell growth rate can contribute to the study of many cellular processes (e.g. growth, the cell cycle, autophagy, apoptosis, cell differentiation) as well as cellular models of disease states. Future versions of this system will provide even more experimental power. It will be possible to simultaneously measure the buoyant mass, volume and density of a trapped growing cell by periodically modulating the solution density within the SMR. In addition, optical access to the trapped cell will allow dynamic cellular and molecular information to be garnered from fluorescent reporters and then correlated in real-time with cell growth.

Supplementary Material

Refer to Web version on PubMed Central for supplementary material.

Acknowledgments

Funding was provided by EUREKA (R01GM085457) and Center for Cell Decision Process Grant (P50GM68762) from the National Institute of Health, and Institute for Collaborative Biotechnologies Grant (DAAD1903D0004) from the U.S. Army Research Office. M.G acknowledges support from Natural Sciences and Engineering Research Council of Canada. F.F.D. acknowledges support from Fundação para a Ciência ea Tecnologia, Portugal, through a graduate fellowship (SFRH/BD/47736/2008). Devices were fabricated at the Massachusetts Institute of Technology's Microsystems Technology Laboratory and at Innovative Micro Technologies.

References

1. Kubitschek HE. J Bacteriol. 1986; 168:613–8. [PubMed: 3536854]
2. Cullum J, Vicente M. J Bacteriol. 1978; 134:330–7. [PubMed: 348686]
3. Reshes G, Vanounou S, Fishov I, Feingold M. Biophys J. 2008; 94:251–64. [PubMed: 17766333]
4. Schaechter M, Williamson JP, Hood JR Jr, Kochal. J Gen Microbiol. 1962; 29:421–34. [PubMed: 13976593]
5. Di Talia S, Skotheim JM, Bean JM, Siggia ED, Cross FR. Nature. 2007; 448:947–51. [PubMed: 17713537]
6. Elliott SG, McLaughlin CS. Proc Natl Acad Sci USA. 1978; 75:4384–8. [PubMed: 360219]
7. Goranov AI, et al. Genes Dev. 2009; 23:1408–22. [PubMed: 19528319]
8. Conlon I, Raff M. Journal of biology. 2003; 2:7. [PubMed: 12733998]
9. Tzur A, Kafri R, LeBleu VS, Lahav G, Kirschner MW. Science (New York, NY). 2009; 325:167–71.
10. Efe JA, Botelho RJ, Emr SD. Curr Opin Cell Biol. 2005; 17:402–8. [PubMed: 15975782]
11. Popescu G, et al. Am J Physiol Cell Physiol. 2008; 295:C538–44. [PubMed: 18562484]
12. Burg TP, et al. Nature. 2007; 446:1066–9. [PubMed: 17460669]
13. Chen KC, et al. Mol Biol Cell. 2004; 15:3841–62. [PubMed: 15169868]
14. Raj A, van Oudenaarden A. Cell. 2008; 135:216–26. [PubMed: 18957198]
15. Prescott DM. Exp Cell Res. 1955; 9:328–37. [PubMed: 13262045]
16. Reshes G, Vanounou S, Fishov I, Feingold M. Physical biology. 2008; 5:46001.
17. Tyson JJ, Hannsgen KB. J Math Biol. 1985; 22:61–8. [PubMed: 4020305]
18. Jorgensen P, Tyers M. Curr Biol. 2004; 14:R1014–27. [PubMed: 15589139]
19. Godin M, Bryan AK, Burg TP, Babcock K, Manalis SR. Applied Physics Letters. 2007; 91:23121.

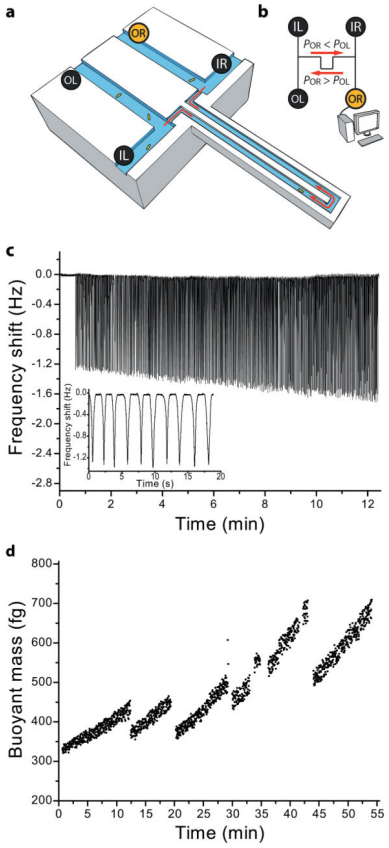

Figure 1.

Dynamic trapping of single cells. (**a**) Illustration of the suspended microchannel resonator (SMR) trapping a single cell. Embedded channel cross-sections for bacteria, yeast and mammalian L1210 mouse lymphoblasts are 3 × 8 microns, 8 × 8 microns, and 15 × 20 microns, respectively. The silicon walls are opaque except in the 15 × 20 microns device, which has thinner walls. (**b**) Schematic of fluidics: sample is injected in parallel through the left and right inlets (IL and IR) and collected at the left and right outlets (OL and OR). While trapping, IL, IR and OL are kept at the same constant pressure; variable pressure at OR applied by a computer controlled regulator determines the direction of fluid flow in the device. (**c**) Raw data showing 400 measurements of one *B. subtilis* cell's buoyant mass. The frequency shift increase with time indicates cellular growth. **inset** Detail of a few peaks that show a locally stable baseline forms after each pass through the SMR, allowing for drift compensation. (**d**) Several *B. subtilis* cells were sequentially trapped. Each point represents the amplitude of the frequency shift, converted to buoyant mass, as the cell transits through the cantilever. Each set of points (e.g. from 0 to 12 minutes) is one single cell or non-segregated cells. Heavier cells have higher growth rates.

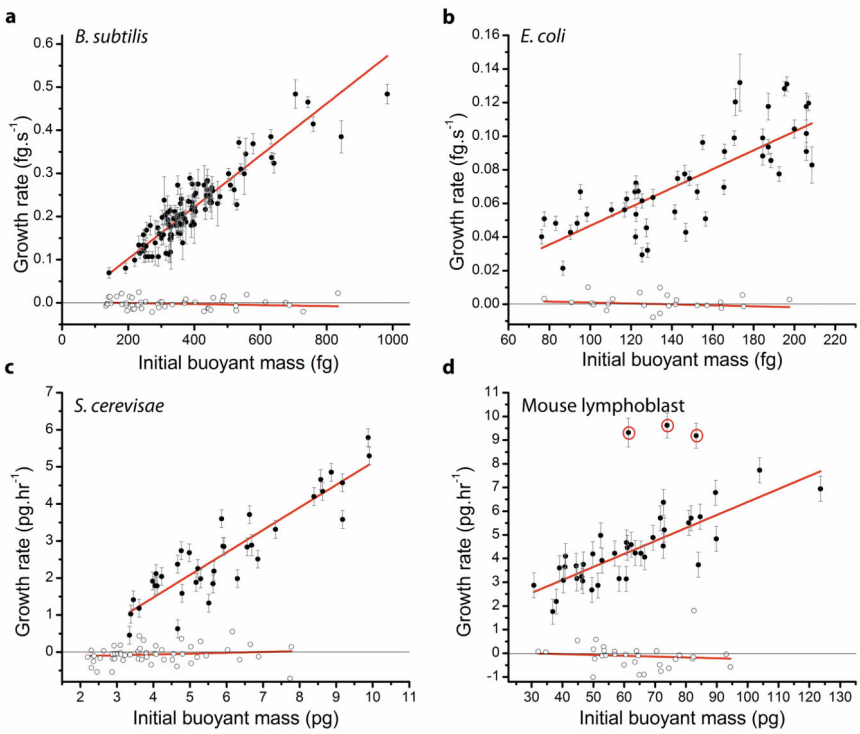

Figure 2.

Growth rate *versus* initial buoyant mass. Each data point represents a trapped cell and is plotted on the diagram according to the cell's initial buoyant mass and the measured growth rate during the trapping period. Filled circles indicate normal growing cells and open circles indicate fixed cells. (**a**) *B. subtilis* (Marburg strain) from 9 cultures grown at 37 °C. (**b**) *E. coli* K12 from 11 cultures grown at 37 °C. (**c**) *S. cerevisiae* from one culture grown at 30 °C. (**d**) L1210 mouse lymphoblasts from two cultures grown at 37 °C. Curve fits are weighted linear regressions. The growth rate errors bars for the growing cells are ± one standard deviation of the growth rate measurements of the fixed cells, except in the cases when the least squares fitting parameter standard error is greater (due to particularly short trapping times). See Online Methods and Supplementary Table 1 for details on culture growth conditions, statistical analysis and experimental errors. Supplementary Figure 6 shows a small, but non-zero, probability of over- or under-determining the growth rate. In light of this, the three L1210 cells that exhibited surprisingly high growth rates (circled in red) were not included in the linear regression.

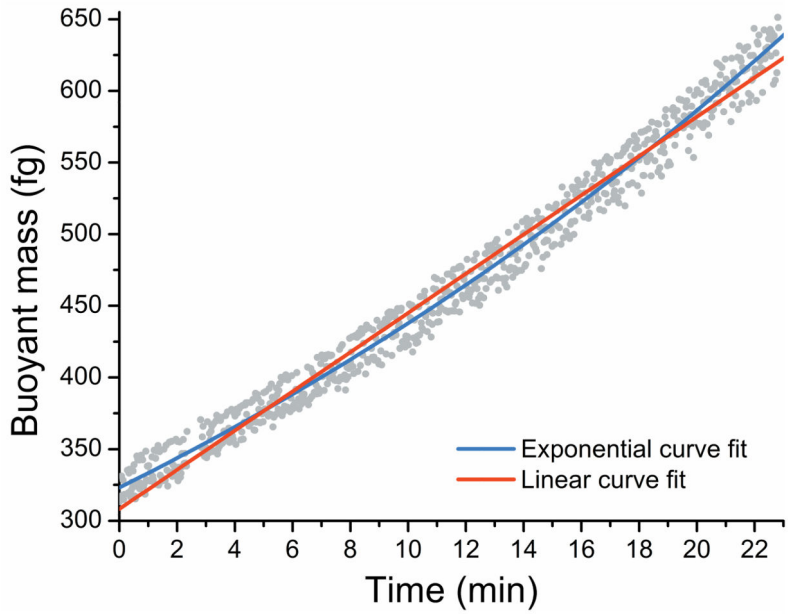

Figure 3.

B. subtilis cell trapped for a period similar to the cell cycle duration. Data is fitted to linear (red; reduced $\chi^2 = 0.00257$) and exponential (blue; reduced $\chi^2 = 0.00187$) functions. See the Supplementary Note and Supplementary Table 4 for details of the statistical analysis, additional models and model comparison.